Cell Biol Toxicol (2025) 41:82
https://doi.org/10.1007/s10565-025-10029-3

RESEARCH

ELF4 improves sepsis-induced myocardial injury by regulating STING signaling-mediated T cells differentiation

Yawen Zheng · Xiongjun Peng · Yusha Zhang · Ruilin Liu · Junke Long

Received: 15 November 2024 / Accepted: 13 April 2025

Abstract Septic cardiomyopathy (SCM) is a common complication caused by sepsis. T cells differentiation is involved in SCM progression. However, the role and underlying mechanisms of T cells-mediated immunity in SCM remain unclear. This study aimed to investigate the role of STING-mediated T cells differentiation in SCM. Cecal ligation and puncture (CLP) surgery was conducted in mice to establish SCM model. The mice were injected intraperitoneally with STING agonist ADU-S100 and C-176 after modeling. Wild type (WT) mice and CD4-STING$^{-/-}$ mice were employed. Besides, overexpressing vectors of ELF4 (oe-ELF4), short hairpin RNA targeting ELF4 (sh-ELF4) were transfected into 293T cells. STING signaling was found to be activated in sepsis-induced myocardial immune injury in mice. The administration of ADU-S100 exacerbated myocardial injury and inflammation, while C-176 alleviated these effects. Additionally, STING activation influenced T cells differentiation, with an increase in Th1 and Th17 cells and a decrease in Treg cells. Conditional knockout of STING in CD4$^+$ T cells reduced Th1 and Th17 populations and improved myocardial function and histology. Furthermore, ELF4 was found to inhibit STING activation, reducing T cells differentiation into pro-inflammatory subsets. Overexpression of ELF4 in CD4$^+$ T cells ameliorated myocardial damage and improved cardiac function in CLP mice, suggesting that the ELF4-STING signaling axis plays a protective role in sepsis-induced myocardial injury by regulating T cells differentiation.

Highlights 1. Activation of STING signaling pathway exacerbated sepsis-induced myocardial injury in mice.
2. STING signaling enhanced pro-inflammatory T cells differentiation and contribute to sepsis-induced myocardial damage in mice.
3. ELF4 directly interacted with STING and negatively regulated its activation.
4. Overexpression of ELF4 ameliorated myocardial injury by regulating STING mediated T cells differentiation.

Y. Zheng
National Clinical Research Center for Geriatric Disorders, Xiangya Hospital of Central South University, Changsha City, Hunan Province, China

X. Peng
Department of Social Affairs, The Second Xiangya Hospital of Central South University, Changsha City, Hunan Province, China

Y. Zhang · J. Long (✉)
Department of Cardiovascular Medicine, The Second Xiangya Hospital of Central South University, No. 139, Middle Renmin Road, Furong District, Changsha City 410011, Hunan Province, China
e-mail: long_junke_Ljk@163.com

R. Liu
Department of Cardiac Surgery, The Second Xiangya Hospital of Central South University, Changsha City, Hunan Province, China

Published online: 07 May 2025

Keywords Septic cardiomyopathy · T cells differentiation · STING · ELF4

Abbreviations

SCM	Septic cardiomyopathy
TBK1	TANK-binding kinase 1
IRF3	Interferon regulatory factor 3
IFN-I	I interferons
ETS	E26 transformation specific
ELF4	E74-like factor 4
MFF	Myeloid elf-1-like factor
CLP	Cecal ligation and puncture
LVEF	Left ventricular ejection fraction
LVFS	Left ventricular fractional shortening
LVESD	Left ventricular end-systolic dimension
HE	Hematoxylin-eosin
FBS	Fetal bovine serum
Co-IP	Co-immunoprecipitation
ELISA	Enzyme-linked immunosorbent assay
IL- 6	Interleukin-6
TNF-α	Tumor necrosis factor-α
CCK- 8	Cell counting kit 8

Introduction

Sepsis is a critical life-threatening syndrome induced by trauma and infection, recently redefined as organ dysfunction caused by a dysregulated host response to infection (Chen et al. 2023; Gu et al. 2020). Statistical data indicated 48.9 million new cases of sepsis worldwide in 2017, with approximately 11 million patients succumbing to sepsis, and suggested that the global burden of sepsis will escalate due to an ageing population (Rudd et al. 2020). Myocardial injury is one of the most common complications of sepsis, and the mortality rate of patients is as high as 30–70%, which is 2–3 times higher than that of patients with non-heart-related sepsis (Kuroshima et al. 2024). However, the pathogenesis of sepsis-induced myocardial injury, commonly referred to as septic cardiomyopathy (SCM), is complex and not fully understood. T lymphocytes, as key components of the immune response, play a vital role in fighting infections (Niu et al. 2018). Moreover, the differential activation and differentiation of T cells are recognized as crucial factors in the progression of sepsis (Heidarian et al. 2023; Chaturvedi et al. 2021). Therefore, investigating the functions and activation mechanisms of T cells holds great promise for uncovering the underlying mechanisms of SCM and potentially improving the immune function of SCM patients.

Stimulator of interferon gene (STING), also known as MYPS, MITA, or ERIS, is a 379 amino acid protein localized predominantly in the endoplasmic reticulum in various human immune cells such as macrophages, T lymphocytes, dendritic cells, and endothelial cells (Chen et al. 2022a). Under physiological conditions, STING exists in a self-inhibited dimeric state that can be activated upon pathogen invasion or cellular damage, resulting in its translocation to Golgi endoplasmic reticulum interface to mediate the activation of TANK-binding kinase 1 (TBK1) and interferon regulatory factor 3 (IRF3), thereby triggering the transcription of type I interferons (IFN-I) and inflammatory cytokines (Oser et al. 2019). Research has shown that activation of the STING-IRF3 signaling cascade exacerbated LPS-induced stimulation of the NLRP3 pathway, thereby contributing to cardiac dysfunction, apoptosis, and pyroptosis (Li et al. 2019). Suppression of the cGAS-STING axis has been shown to significantly mitigate LPS-induced cardiac dysfunction, inflammation, and apoptosis (Liu et al. 2023). Additionally, STING has been implicated in exacerbating endotoxin-induced $CD4^+$ T cells parthanatos by stimulating PARP- 1 activity during acute systemic inflammation (Luan et al. 2022; Long, et al. 2020). Moreover, studies in cancer and inflammatory diseases have linked STING pathway activation to the modulation of various T cells subsets (Jneid, et al. 2023; Imanishi et al. 2014). In light of these evidences, the precise role of STING in regulating myocardial injury during sepsis warrants further investigation.

The E26 transformation specific (ETS) transcription factor family comprises 29 members, each characterized by a conserved DNA-binding domain (5'-GGAA) that allows ETS recognition of core consensus sequences (Tyler et al. 2021). E74-like factor 4 (ELF4), a member of ETS transcription factor family, was reported to be a pivotal regulator in human autoinflammatory diseases through affecting several aspects of the immune response including NK cells development, $CD8^+$ T cells proliferation and Th17 cells differentiation (Tyler et al. 2021). Cao et al. also showed that ELF4 inhibited inflammatory Th17 cells

activity by promoting IL1RN transcription, thereby inducing macrophage M2 polarization and alleviating inflammatory bowel disease (Cao et al. 2023). Significantly, You et al. revealed that ELF4 served as a IFN-I transcription factor, instrumental in modulating IFN-I response and antiviral defense (You et al. 2013), underscoring the critical role of ELF4 in orchestrating the body's immune response. Despite these insights, the involvement of ELF4-mediated immune regulation in the pathogenesis of sepsis and related complications remains an open question that warrants further investigation.

Previous research has demonstrated that ELF4 direct interacted with the STING protein to drive interferon synthesis (You et al. 2013). Consistently, computational predictions from GeneMANIA suggested a potential interaction network between ELF4 and STING. In the present study, we provide novel evidence that ELF4 directly interacted with STING protein to block the phosphorylation of TBK1, which in turn ameliorated sepsis-induced cardiac dysfunction and myocardial injury by modulating T cells differentiation. These groundbreaking findings elucidated for the first time the molecular mechanism underlying ELF4/STING-mediated T cells immune dysregulation in SCM, paving the way for the development of innovative therapeutic and preventive strategies against this debilitating condition.

Materials and methods

Animals

8-week-old male C57BL/6, CD4-Cre and STING-flox mice were purchased from the Shanghai Model Organisms Center (Shanghai, China). In addition, fifteen CD4-Cre STING-flox (CD4-STING$^{-/-}$) mice strains were generated by crossing STING-flox and CD4-Cre mice, and littermates as control (WT). All mice were housed according to internationally accepted standards, with four animals per cage, under constant ambient temperatures of 22 ± 0.5 °C and strict adherence to a 12-h light/12-h dark photoperiod schedule to maintain their circadian rhythms. Adequate food and water were provided ad libitum. All experimental procedures were granted formal approval by Institutional Animal Care and Use Committee (IACUC) of The Second Xiangya Hospital, Central South University (No. 2021229). The reporting of experimental results strictly adhered to the ARRIVE guidelines to ensure transparency and reproducibility of the study. Investigators were blind to animal treatments, no adverse effects were observed during these studies, and all animals were included in statistical analyses.

Constructive of sepsis mouse model

According to experimental design, the groups were as follows: Sham, CLP + WT, CLP + CD4-STING. C57BL/6 mice were randomly divided into two groups including sham and CLP. In addition, C57BL/6 mice, WT mice and CD4-STING$^{-/-}$ mice were subjected to cecal ligation and puncture (CLP) surgery. There were 15 mice in each group. As previously described (Imbaby and Hattori 2023), mice were anesthetized via inhalation of 3–4% isoflurane administered via a mid-abdominal incision. Ibuprofen (250 μg/mL in drinking water) was used for pre- and post-operative analgesia. Mobilization, ligation, and double puncture of the cecum were accomplished using a 21-gauge needle, followed by gentle extrusion of a small amount of fecal content. Subsequently, the cecum was repositioned and sutured back into the abdomen. Mice in sham group underwent identical surgical techniques, except that the cecum was exposed but neither ligated nor punctured. Immediately following surgery, all mice received a subcutaneous injection of 0.5 mL of sterile saline solution. To activate or block STING signaling in C57BL/6 mice, mice were injected intraperitoneally with 50 μg/g ADU-S100 (MedChemExpress, Monmouth Junction, NJ, USA) or 30 μg/g C176 (MedChemExpress) at 1 h and 12 h after CLP operation (Berger et al. 2022; Wu et al. 2022). Post-operation for 24 h, coronary blood and heart tissue samples were collected for further analysis. All mice were euthanasia by administrating with excessive phenobarbital sodium (Sigma-Aldrich, St. Louis, MO, USA). Two dead mice were excluded, and five mice in each group were selected for subsequent analysis.

Echocardiography

Before euthanizing the mice, cardiac function was assessed in the mice using low-frequency imaging transducers for transthoracic echocardiography

(VEVO 2100, Visual Sonics). In short, mice were anesthetized with 2% isoflurane, and a sequence of M-mode images were obtained at the level of the papillary muscles. Transthoracic echocardiography was used to measure left ventricular ejection fraction (LVEF), left ventricular fractional shortening (LVFS), and left ventricular end-systolic dimension (LVESD).

Histopathological staining

Fresh heart tissues were ere fixed with 4% paraformaldehyde for overnight, and embedded in paraffin, and 5 μm-thick sections were then cut perpendicularly. Hematoxylin–eosin (HE) staining was performed using a hematoxylin–eosin staining kit (Beyotime, Shanghai, China), with sections stained for 5 min with hematoxylin and 1 min with eosin, both at room temperature. Masson staining was also performed by utilizing a Masson staining kit (Solarbio, Beijing, China) in line with manufacturer's instructions. All experimental slides were viewed using a BX43 optical microscope (Olympus, Tokyo, Japan).

Flow cytometry

At 24 h post-CLP, coronary blood samples were obtained from the mice in each group by cardiac puncture. Then, the measurement of T cells number and differentiation were performed by flow cytometry according to a previous study (Chen et al. 2023).

Briefly, we obtained hearts peripheral blood mononuclear cells (PBMCs) using Ficoll density gradient centrifugation within 6 h of blood collection. Then, these isolated PBMCs were then cryopreserved for later testing and analysis. An BD FACSAria™ Fusion (BD Biosciences, San Jose, CA, USA) was used to sorted $CD4^+$ T cells and $CD8^+$ T cells. To obtain the proportion of $CD4^+$, $CD8^+$, B cells and non-lymphocyte, PBMCs washed with fluorescence-activated cell sorting (FACS) buffer and then stained for 30 min at room temperature in the dark with fluorescent-labeled anti-mouse monoclonal antibodies: CD3-PE (ab22268, Abcam, Cambridge, MA, USA), CD4-FITC (ab269349, Abcam), CD8-FITC (ab237367, Abcam) or their respective isotype controls. Fluorescence was evaluated by flow cytometry. Besides, to achieve the proportion of Th1, Th17, and Treg cells in $CD4^+$ T cells, flow cytometry was used. Firstly, the isolated $CD3^+CD4^+$ T cells were further stained with IFN-γ-APC (ab210390, Abcam), a Th1 marker, to label Th1 cells for 30 min. The isolated $CD3^+CD4^+$ T cells were further stained with IL-17-FITC (ab210240, Abcam, Th17 marker), a Th17 marker, to label Th17 cells for 30 min. The isolated $CD3^+CD4^+$ T cells were further stained with FOXP3-FITC (ab210230, Abcam), a Treg marker, to label Treg cells for 30 min. Isotype control antibodies and fluorescence minus one (FMO) control were used as controls in experiments. A BD FACSCelesta™ flow cytometer (BD Biosciences, San Jose, CA, USA) was used to detect the proportion of those cells. All data were analyzed with FlowJo software (Tree Star, Ashland, OR 97520, USA).

Cell culture, cell transfection treatment and adoptive transfer

The spleen of normal C57BL/6 mice (8 weeks old) was quickly cut and ground into single cell suspension. The single cell suspension was then resuspended by using a 70 μm cell filter. Untouched $CD4^+$T cells were magnetically isolated using EasySep™ Mouse $CD4^+$T Cells Isolation Kit (#19852, STEMCELL Technologies, Grenoble, France) Purity of the isolate $CD4^+$cells constantly exceeded 95%. Naïve primary mouse $CD4^+$T cells were cultured in RPMI 1640 medium containing 10% T-cell culture supplement with Con A (T-STIM with Con A, BD Biosciences) and 10% FBS.

For cell transfection, the lentivirus, the lentivirus-packed overexpressing vectors of ELF4 (oe-ELF4), empty vector (oe-NC), short hairpin RNA targeting ELF4 (sh-ELF4) and sh-NC were obtained from GenePharma company (Shanghai, China). The above lentivirus particles (10 μL, 10^7 TU/mL) were infected into 293T cells, and the transfection efficiency was detected after transfection for 48 h. The control group was transfected with empty virus vector.

T cells were labeled with 5 μM CFSE(Invitrogen) and injected intravenously into C57BL/6 mice (10^4 cells/mouse) (Lee et al. 2020).

Real-time quantitative PCR (RT-qPCR)

Total RNA was extracted using Trizol reagent (Invitrogen, USA), and the collected RNA was reverse transcribed into cDNA using a Prime-ScriptTM one step RT-qPCR kit (Takara Bio, China). RT-PCR was

performed using a PrimeScript RT reagent Kit on an ABI7900 Real-Time PCR System (Applied Biosystems, USA). The relative expressions of genes were normalized to GAPDH, and the relative quantitative analysis was conducted using $2^{-\Delta\Delta CT}$ method. Primers sequences used were as follows: STING forward 5′-GGCGTCTGTATCCTGGAGTA- 3′, reverse 5′-TAGACAATGAGGCGGCAGTTAT- 3′; GAPDH forward 5′- AGGTCGGTGTGAACGGATTTG- 3′, reverse 5′- GGGGTCGTTGATGGCAACA- 3′;

Western blot

The proteins were obtained from heart tissues and $CD4^+$ T cells by using RIPA buffer (Beyotime) containing protease inhibitors and the concentration was subsequently evaluated by a BCA kit (Beyotime). An equal amount of protein (20 μg) was loaded onto a 12% polyacrylamide gel for SDS-PAGE, and subsequently transferred to a PVDF membrane (Millipore, Billerica, MA, USA). The PVDF membrane was then blocked with 5% non-fat milk and incubated with primary antibodies against ELF4 (ab96075, Abcam), STING (ab288157, Abcam), p-TBK1 (PA5 - 105,919, Invitrogen), TBK1 (PA5 - 17,478, Invitrogen), and β-actin (ab8226, Abcam) overnight. Following this, the membrane was incubated with a secondary antibody for an additional 60 min. Protein bands were visualized using an ECL detection kit (Bio-Rad, Munich, Germany) and the band intensities were quantified using ImageJ software.

Co-immunoprecipitation (Co-IP)

The protein interplay between ELF4 and STING was measured using Co-IP assay via an immunoprecipitation kit (Sangon Biotech, Shanghai, Chian). Briefly, 293T cells were lysed, and the cell lysates were incubated with magnetic bead-conjugated antibodies targeting ELF4 (#ELF4-BIOTIN, Fabgennix, Frisco, TX, USA), STING (ab288157, Abcam), TBK1 (ab109735, Abcam), IRF3 (ab76409, Abcam) or IgG (ab6789, Abcam) for a duration of 12 h at 4 °C. Subsequently, the beads were retrieved, thoroughly washed, and the immunoprecipitated proteins were denatured in SDS loading buffer before being subjected to western blot analysis for further examination of the target proteins.

Enzyme-linked immunosorbent assay (ELISA)

The levels of cytokines including Interleukin- 6 (IL-6), Interleukin-12 (IL-12), Interleukin-10 (IL- 10), Interleukin-1β (IL-1β) and Tumor necrosis factor-α (TNF-α) in heart tissues and coronary blood from mice were evaluated by ELISA. In short, heart tissues were obtained from mice and then were homogenized and centrifuged to obtain supernatant and cardiomyocytes were centrifuged to obtain supernatant. Blood samples were centrifuged to obtain serum. According to corresponding experimental procedure of manufacture's protocol, the levels of cytokines factors were detected by means of ELISA kits (Beyotime). The final optical density (OD) value was recorded by microplate reader (Thermo Fisher Scientific, Waltham, MA, USA), and the concentrations of cytokines were calculated according to the corresponding standard curve.

Statistical analysis

All animal experiments were independently replicated five times, whereas cellular assays were repeated a minimum of thrice. Data analyses were executed using GraphPad Prism version 8.0. Results were presented as mean ± standard deviation (Mean ± SD). Prior to statistical testing, normality and homogeneity of variance were confirmed by Kolmogorov–Smirnov test. In this study, one-way ANOVA followed by Tukey's post hoc test was used for multiple group comparisons. Statistical significance was set at $p < 0.05$.

Result

CLP mice exhibit augmented STING activation in SCM

To investigated the role of STING signaling pathway in SCM, we conducted CLP to mimic SCM as described before (Long, et al. 2020). Echocardiography showed reduced LVEF and LVFS but enhanced LVESD in CLP group compared to sham group as reported in many studies (Fig. 1A**,** Table 1). In addition, histological staining also revealed severe myocardial damage, including massive cell necrosis and obvious inflammatory infiltration in CLP myocardial (Fig. 1B). Subsequently, the expression of STING and its related pathways proteins TBK1,

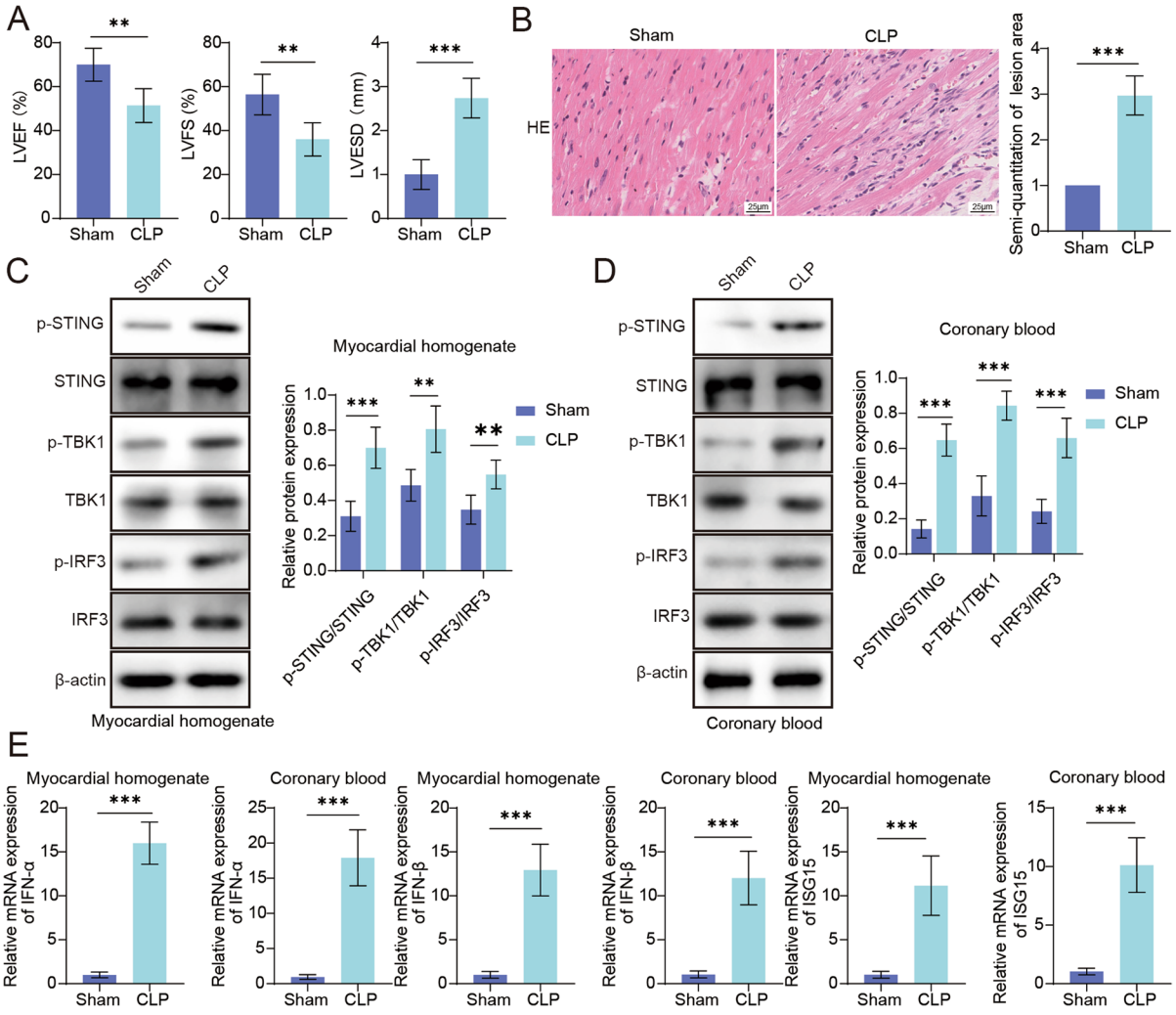

Fig. 1 CLP mice exhibit augmented STING activation in SCM. C57BL/6 mice was subjected to CLP surgery to conduct a septic mouse model. **A**. Echocardiography was used to evaluate cardiac function parameters (LVEF, LVFS, LVESD). B. Representative images stained by HE for assessing the pathologic changes. **C**-**D**. Western blot analysis evaluated the protein levels of STING, p-STING, TBK1, p-TBK1, IRF3 and p-IRF3. E. RT-qPCR analysis determined the mRNA levels of IFN-α, IFN-β and ISG15. Data was shown as mean ± SD. N = 5. **p < 0.01, ***p < 0.001

Table 1 Echocardiographic properties feature of Fig. 1 experimental mice

	Sham	CLP
Heart rate (bpm)	465 ± 5.70	475.2 ± 5.93
LV EF (%)	70 ± 7.52	51.40 ± 7.73
LV FS (%)	56.4 ± 9.24	36 ± 7.58
LV ESD (mm)	1 ± 0.34	2.74 ± 0.45
Calculated LV mass (mg)	92.5 ± 1.99	88.18 ± 5.56

p-TBK1, IRF3 and p-IRF3 in myocardial tissues and coronary blood were detected using Western blot analysis. Compared with the sham group, STING/TBK1/IRF3 pathways were significantly activated in CLP group mice both in myocardial tissue and coronary blood (Fig. 1C-D). In line with this, RT-qPCR results showed significantly increased expression of IFN-α, IFN-β and ISG15 in myocardial tissues and coronary blood of CLP group mice compared to the sham group (Fig. 1E). These results indicating the critical role of STING in SCM.

Activation of STING aggravated sepsis-induced myocardial damage

To investigate whether STING signaling is involved in SCM, the agonist (ADU-S100) or antagonist (C-176) of STING was administered to activate or inhibit STING signaling in CLP mice (Fig. 2A). Echocardiography and H&E results showed ADU-S100 treatment significantly exacerbated damage of heart in CLP mice. However, C-176 treatment rescued these influences of CLP surgery (Fig. 2B, C**,** Table 2). Consistently, it was observed that the pro-inflammatory cytokines in myocardial tissues and coronary blood from CLP group mice including IL-6, IL-12, IL-1β and TNF-α were dramatically enhanced and anti-inflammatory factor IL-10 was inhibited compared to the sham group, and these changes were strengthened after ADU-S100 treatment, but ameliorated by C-176 treatment (Fig. 2D). In summary, activation of STING is responsible for myocardial damage, dysregulation of cardiac function and inflammation in SCM.

STING activation promoted T cells enrichment in SCM

To clarify what immunocyte subset is responsible for STING-regulated SCM, T cells, B cells and non-lymphocyte were sorted by flow from coronary blood samples by cardiac puncture, then the expression and activation of STING signaling were detected. Western blot suggests much higher activation of STING in T cells than other subsets, indicating T cells was involved in STING-regulated SCM (Fig. 3A). Further, flow results showed increased T cells frequency, interestingly no significantly change was observed in B cells or non-lymphocyte (Fig. 3B). T cells subsets, especially Th1/17 and Treg have been involved in SCM in several studies, so we detected the frequency of these T cells subsets (Fig. 3C). To figure out the role of STING in T cells distribution, we utilized ADU-S100 or C-176 to agonist or antagonist STING in CLP mice and T cells subsets in coronary blood were detected by flow. As depicted in Fig. 3D, CLP mice displayed remarkable increasement of $CD4^+$T and $CD8^+$T cells, which was promoted by ADU-S100 treatment but reversed by C-176 intervention (Fig. 3D). Similarly, the increased populations of Th1 and Th17 were reinforced by ADU-S100 treatment, but abolished by C-176 administration, indicating STING may regulate SCM by T cells differentiation (Fig. 3E). In conclusion, the activation of STING activation facilitated T cells enrichment in SCM.

STING promoted T cells differentiating into Th1/17

To delve deeper into the role of STING in T-cells differentiation in SCM, $CD4^+$ T cells-specific STING conditional knockout (CD4-$STING^{-/-}$) mice were subjected to CLP surgery, and $STING^{f/f}$ littermatesas control (WT). In relative to WT group, CD4-$STING^{-/-}$ mice showed reduced expression of STING in $CD4^+$ T cells, but no change in $CD8^+$ T cells (Fig. 4A). Additionally, CD4-$STING^{-/-}$ mice exhibit reduced Th1 and Th17 frequency and increased Treg frequency in coronary blood under CLP surgery (Fig. 4B). Likewise, the elevated frequency of Th1 and Th17 cells and the reduced Treg cells ratio in spleen also were reversed in CD4-$STING^{-/-}$ mice (Fig. 4C), this universal change suggests that STING may regulate Th1/17 frequency through T cells differentiation. To verify this suspicion, we isolated Naïve $CD4^+$T cells from WT or CD4-$STING^{-/-}$ mice for T cells differentiation test under indicating cytokine panel. $STING^{-/-}$ $CD4^+$ T cells displayed extremely lower ability differentiating into Th1/17 but augmented Treg differentiation (Fig. 4D). In addition, the elevated levels of IL-6, IL-1β, IL-12 and TNF-α and reduced IL-10 level in heart tissues were rescued by STING knockout in $CD4^+$T cells (Fig. 4E). Simultaneously, H&E staining showed reduced inflammatory infiltration in myocardial tissues, elevated LVEF/LVFS and decreased LVESD upon CLP surgery in CD4-$STING^{-/-}$ mice (Fig. 4F, G**,** Table 3). To sum up, STING deficiency in $CD4^+$T cells may ameliorate SCM via regulating T cells differentiation.

ELK4 interacted with STING to inhibit the activation of STING in $CD4^+$ T cells

Here, through searching GeneMANIA database, we predicted that ELF4 potentially interacts with STING. Then, we proceeded to experimentally verify the putative binding interaction between ELF4 and STING. As shown in Fig. 5A, Co-IP experiments exhibited significant interaction between ELF4 and STING in 293T cells, and further data suggests this interaction was in a concentration-dependent manner

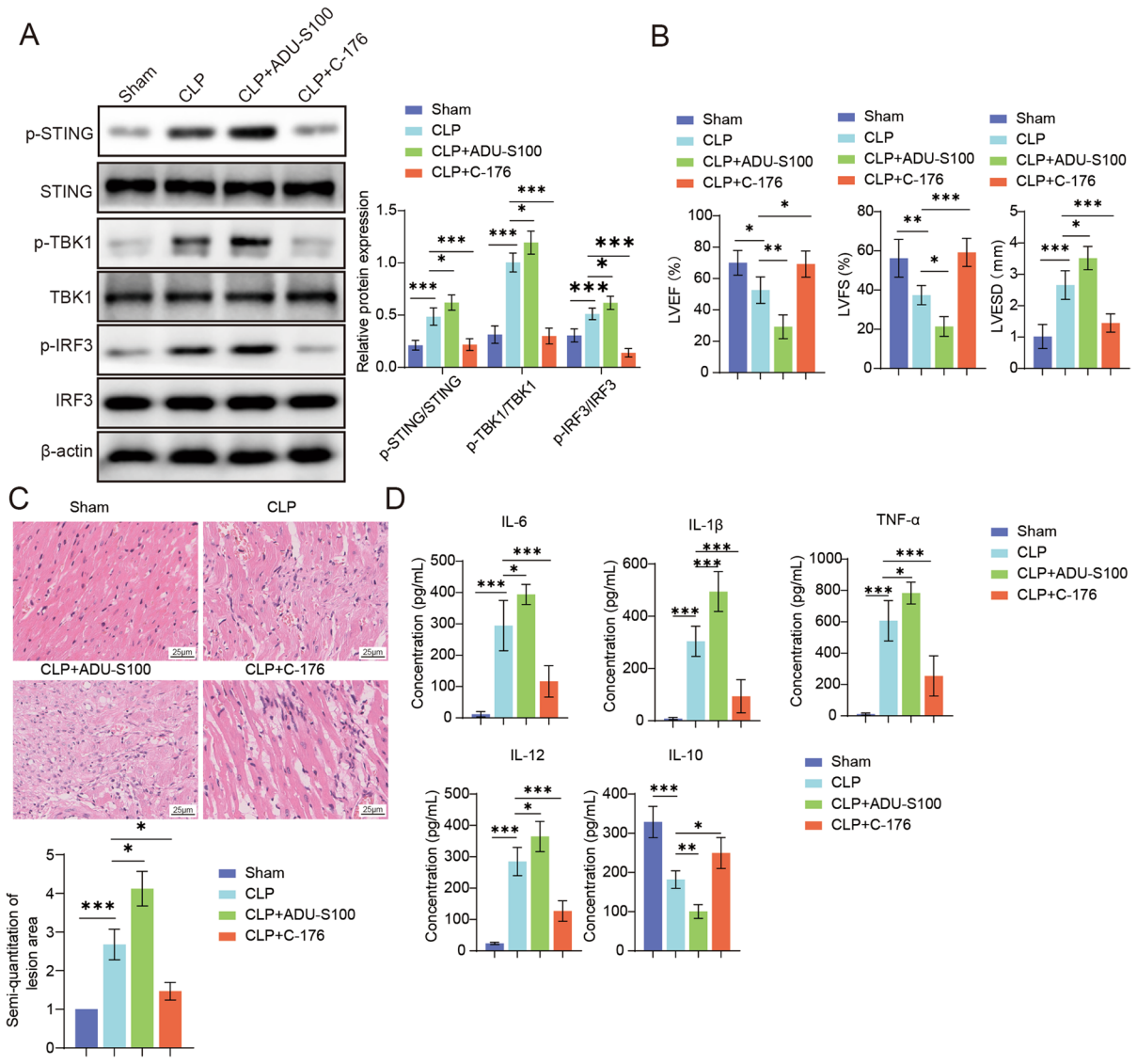

Fig. 2 Activation of STING aggravated sepsis-induced myocardial damage. C57BL/6 mice was subjected to CLP surgery to conduct a septic mouse model. The STING agonist (ADU-S100) and STING antagonist (C-176) were administrated at 1 h and 12 h after CLP operation. Mice in each group were sacrificed 24 h after CLP. The coronary blood samples were acquired from each group mice. **A**. The protein levels of STING, p-STING, TBK1, p-TBK1, IRF3 and p-IRF3 were evaluated by western blot analysis. **B**. Cardiac function parameters (LVEF, LVFS, LVESD) were examined by Echocardiography. **C**. Representative images stained by HE for assessing the pathologic changes. **D**. ELISA analysis was performed for quantifying the levels of IL-6, IL-12, IL-1β, TNF-α and IL-10. N = 5. Data was shown as mean ± SD. *p < 0.05, **p < 0.01, ***p < 0.001

(Fig. 5B), indicating that their binding becomes more pronounced as ELF4 expression levels rise. However, ELF4 did not interact with TBK1 or IRF3 (Fig. 5C, D). Moving forward, we further explored the impact of ELF4 on STING in vitro. Firstly, we successfully overexpressed or knocked down ELK4 expression in 293T cells through transfecting with oe-ELF4 or sh-ELF4, as determined by western blot. We also noticed that overexpression of ELF4 repressed STING activation, while knocking down ELF4 promoted STING activation (Fig. 5E). Additionally, the expression and localization of STING and ELF4 expression in

Table 2 Echocardiographic properties feature of Fig. 2 experimental mice

	Sham	CLP	CLP + ADU-S100	CLP + C- 176
Heart rate (bpm)	465.2 ± 6.42	475.4 ± 6.19	481.6 ± 6.23	469.8 ± 4.21
LV EF (%)	70 ± 7.90	52.60 ± 8.47	29.20 ± 7.60	69.20 ± 8.32
LV FS (%)	56.20 ± 9.60	37.40 ± 4.93	21.40 ± 5.03	59.20 ± 7.16
LV ESD (mm)	1.02 ± 0.38	2.66 ± 0.46	3.52 ± 0.37	1.45 ± 0.29
Calculated LV mass (mg)	93.16 ± 3.24	88.48 ± 5.63	85.28 ± 4.01	89.7 ± 3.02

293T cells was investigated. As presented in Fig. 5F, STING and ELF4 co-localized perinucleus of 293T. Taken together, ELK4 directly interacted with STING to inhibit the activation of STING in 293T cells.

ELF4 overexpression alleviated cardiomyocyte injury by regulating STING signaling-mediated Th1/17 differentiation

To investigate the role of ELF4-STING signaling axis-mediated T cells differentiation in SCM, mouse primary $CD4^+$ T cells were isolated and transfected with overexpressing ELF4 plasmids for differentiation test ex vivo. As demonstrated by Fig. 6A, flow cytometry analysis revealed that the elevation of ELF4 reduced the differentiation of Th1 and Th17 cells in $CD4^+$ T cells and enhanced Treg differentiation. To verify the effects of ELF4-STING signaling axis-mediated T cells differentiation in vivo, naïve Ctl T cells, OE-NC T cells and OE-ELF4 T cells were adoptively transferred into WT mice, followed by CLP surgery. H&E staining of heart tissues illustrated that myocardial injury was mitigated after transplantation of OE-ELF4 T cells into CLP mice (Fig. 6B). Similarly, echocardiography exhibited that the transplantation of OE-ELF4 T cells induced obvious elevation in LVEF and LVFS, and reduction in LVESD (Fig. 6C**,** Table 4). In summary, ELF4 upregulation ameliorated cardiomyocyte injury by regulating STING-mediated T cells differentiation.

Discussion

Excessive inflammation and immune dysregulation are key contributors to sepsis mortality (Poll et al. 2021). T lymphocytes, as a fundamental component of the immune response, pose a significant threat to the prognosis and long-term survival of sepsis patients (Jensen et al. 2018; Huang et al. 2022). T lymphocytes, classified into $CD4^+$ and $CD8^+$ subsets based on surface markers, with their numerical changes and $CD4^+/CD8^+$ ratio closely associated with immune function in sepsis patients (Danahy et al. 2016; Xia et al. 2012; Chen et al. 2022b). Clinical experiments revealed that sepsis led to decreases total $CD4^+$ and $CD8^+$ cells counts and impaired their antigen-driven responsiveness and effector functions (Danahy et al. 2016). Furthermore, an increase in $CD8^+$ T cells effectively reduced the levels of inflammation markers in the blood, thereby increasing the survival rate of sepsis-immune mice (Anyalebechi et al. 2024). Blocking $CD8^+$ T cells apoptosis effectively mitigated the severity of sepsis (Liu et al. 2022). Th1 and Th2 represent two mutually antagonistic subsets of $CD4^+$ T cells and the number of Th1 cells and the levels of their associated secretion of IFN-γ, TNF-α and IL-2 were elevated in the initial stages of murine sepsis (Zhao et al. 2023). Th17 and Treg cells, derived from $CD4^+$ T cells, exerted opposing effects on pro-inflammation and anti-inflammation, respectively. Some evidence has indicated that reducing the number of Th17 cells and increasing the number of Treg cells could alleviate excessive inflammation during the early phase of sepsis and improve sepsis-related injury (Xia et al. 2020; Liu et al. 2020). It can be seen from this evidence that immune dysregulation mechanisms driven by T lymphocytes played a crucial role in diagnosis and therapy for sepsis. However, the immune mechanisms triggered by T lymphocytes in SCM remain unclear. In our study, we are the first proposed that ELF4-mediated STING signaling inhibition ameliorated myocardial damage in SCM by decreasing the number of $CD4^+$ T cells and promoting $CD4^+$ T cells differentiating into Treg rather than Th1 and Th17. These evidences might provide valuable insight for immunotherapeutic strategies targeting SCM.

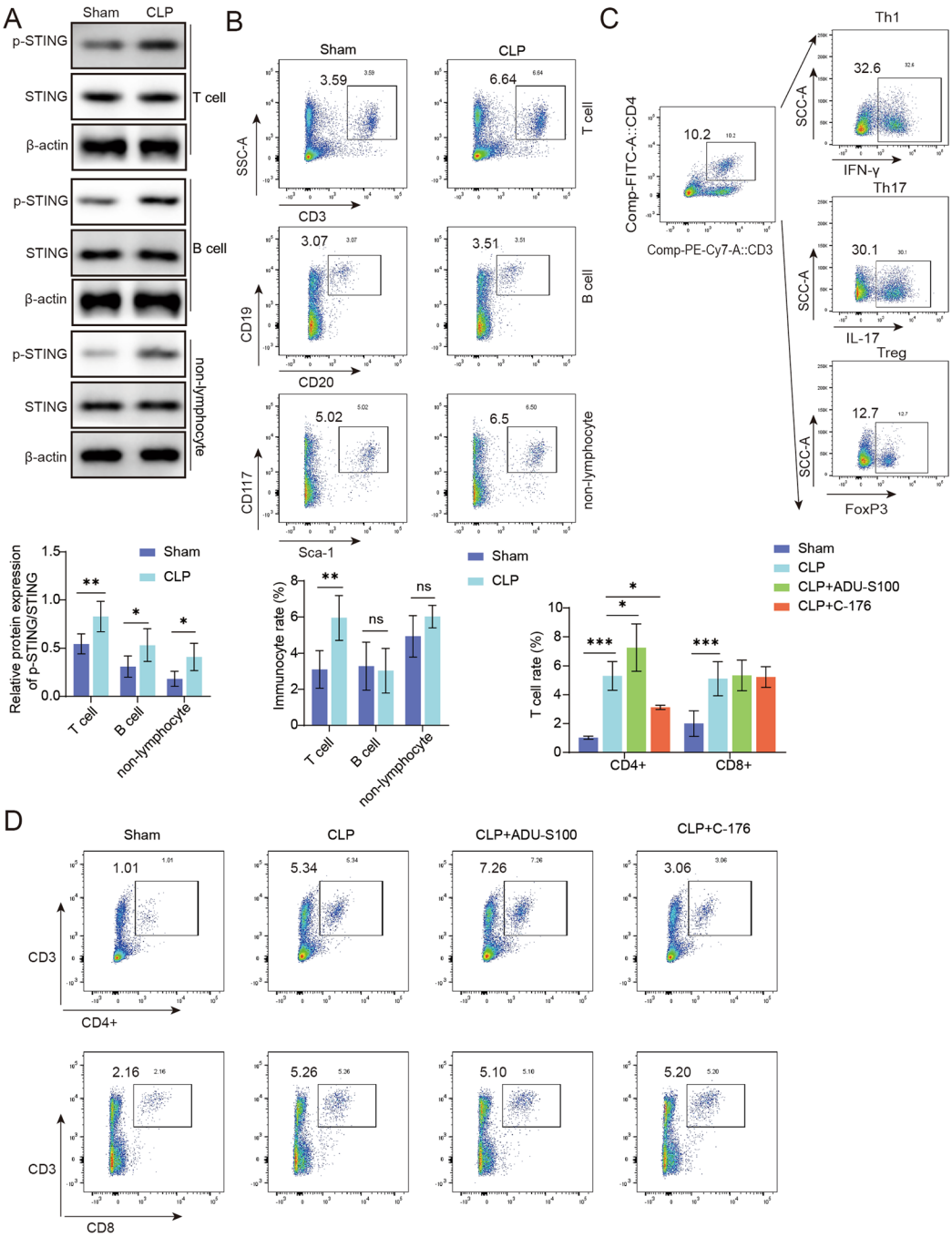

Fig. 3 STING activation promoted T cells enrichment in SCM. C57BL/6 mice was subjected to CLP surgery to conduct a septic mouse model. **A**. The expressions of STING in T cells, B cells and non-lymphocytes in coronary blood were evaluated western blot assay. **B**. The frequency of T cells, B cells and non-lymphocyte in the coronary blood of mice were assessed using flow cytometry. **C**. The differentiation rate of $CD4^+$ T cells toward to Th1, Th17 and Treg cells were analyzed by flow cytometry. D. The STING agonist (ADU-S100) and STING antagonist (C-176) were administrated at 1 h and 12 h after CLP operation. The coronary blood samples were acquired from each group mice. **D**. The overall percentage of $CD4^+$ T cells and $CD8^+$ T cells were quantified by flow cytometry. **E**. The differentiation rate of $CD4^+$ T cells toward to Th1, Th17 and Treg cells were analyzed by flow cytometry. Data was shown as mean ± SD. N = 5. *p < 0.05, **p < 0.01, ***p < 0.001

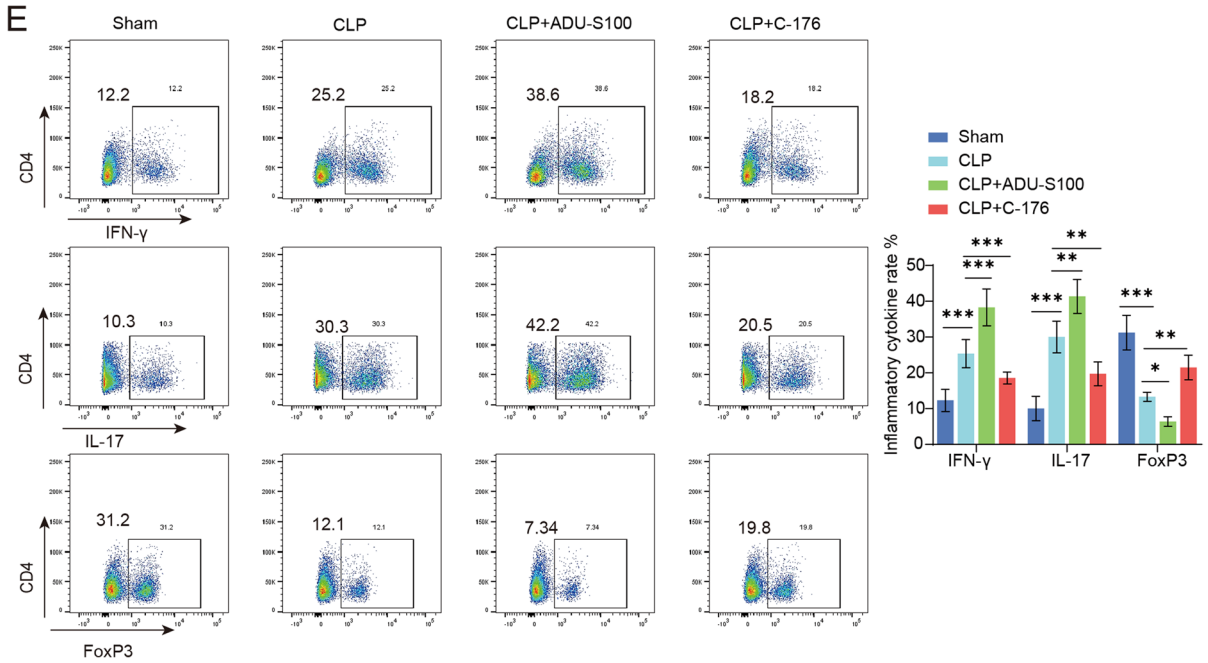

Fig. 3 (continued)

So far, extensive research has demonstrated a strong association between the STING signaling pathway and sepsis. For instance, STING could promote inflammatory responses and exacerbate the lethal coagulopathy accompanying sepsis (Zhang et al. 2020). Besides, a previous study indicated that STING deficiency significantly alleviated cardiac function, myocardial inflammation and myocardial cell death in sepsis mice (Li et al. 2019). Similarly, inactivation of cGAS-STING pathway significantly attenuated myocardial inflammation, oxidative stress, and cardiac dysfunction in septic mice (Liu et al. 2023). In this study, we established an in vivo SCM model using CLP surgery. Our findings revealed that STING agonist ADU-S100 exacerbated CLP-induced cardiac dysfunction, myocardial inflammation. Conversely, STING inhibitor C-176 exerted opposite effects, which were consistent with previous studies. In conclusion, our results suggested that the STING played a crucial role in SCM progression through affecting immune $CD4^+$ T cells.

Additionally, our findings firstly revealed that inhibiting the activation of STING signaling suppressed the number of $CD4^+$ T cells in the hearts of CLP mice, promoting anti-inflammatory Treg populations while concurrently reducing a shift towards pro-inflammatory Th1 and Th17 subsets. Meanwhile, the role of STING signaling in SCM might be linked to T lymphocyte-mediated immune dysregulation. As previously documented, Long et al. demonstrated that STING induced $CD4^+$ T cells apoptosis in acute inflammatory disease (Long, et al. 2020), and also could promote $CD4^+$ T cells parthanatos via regulating PARP-1/PAR activation (Luan et al. 2022). Besides, STING promoted endoplasmic reticulum stress by disrupting intracellular calcium homeostasis, thus leading to senescence and apoptosis of T cells (Wu et al. 2019). Activation of STING signaling also enhanced Th1 differentiation of $CD4^+$ T cells by increasing IFN-γ and IL-9 production (Benoit-Lizon, et al. 2022). Moreover, cGAS-STING signaling activation played crucial role in initiating T cells apoptosis in thymus development (Ratiu et al. 2022). Here, we found that conditional knockdown of STING in $CD4^+$ T cells dramatically ameliorated CLP surgery-induced myocardial inflammation and suppression of the differentiation of $CD4^+$ T cells towards Th1 and Th17 subsets and promoting the expansion of Treg populations in mice. This finding strongly suggested that the STING signaling

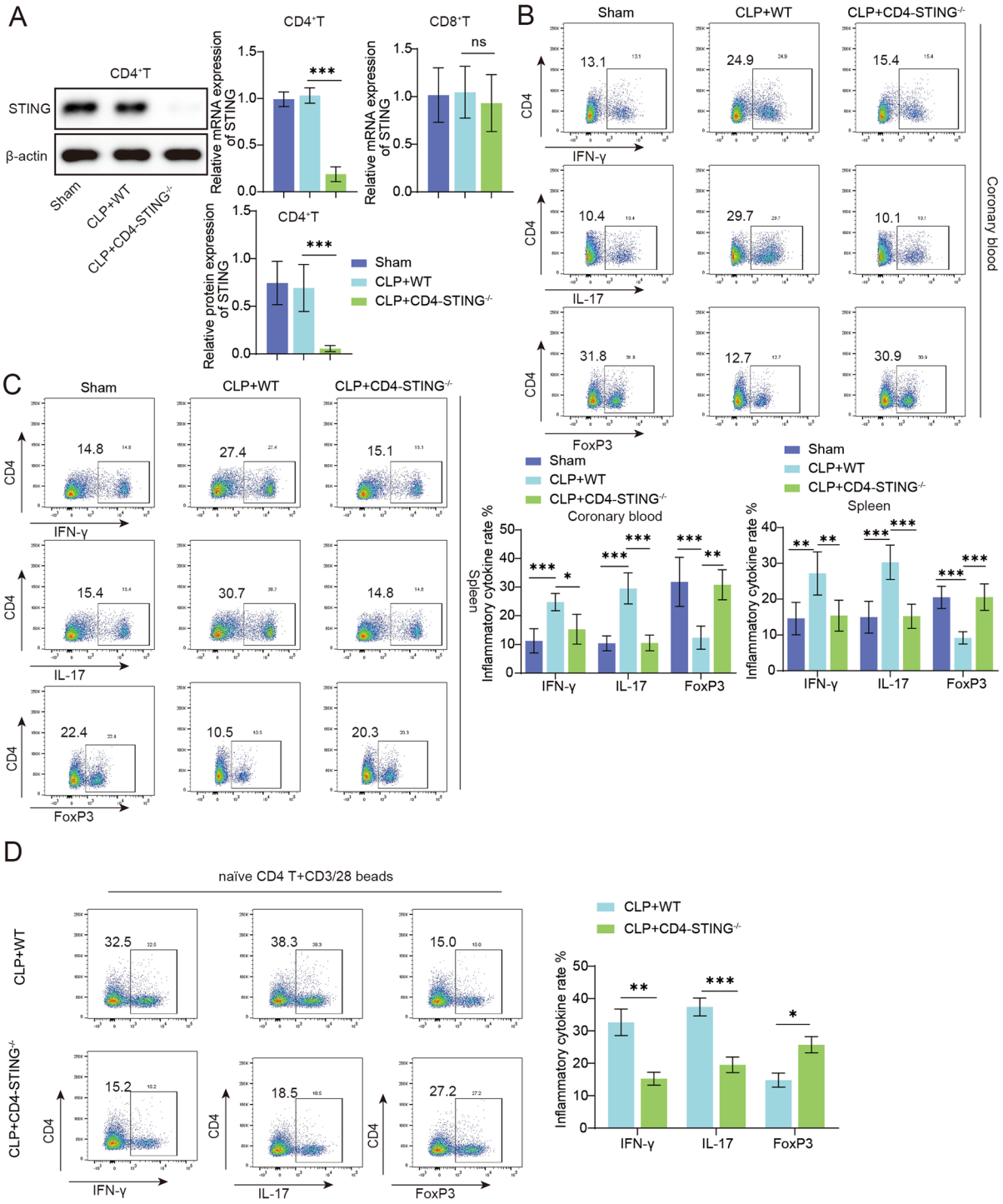
A
CD4+T
STING
β-actin
Sham
CLP+WT
CLP+CD4-STING-/-
CD4+T
Relative mRNA expression of STING
***
CD8+T
ns
Relative mRNA expression of STING
CD4+T
Relative protein expression of STING
***
Sham
CLP+WT
CLP+CD4-STING-/-
B
Sham
CLP+WT
CLP+CD4-STING-/-
13.1
24.9
15.4
10.4
29.7
10.1
31.8
12.7
30.9
CD4
IFN-γ
IL-17
FoxP3
Coronary blood
Sham
CLP+WT
CLP+CD4-STING-/-
Coronary blood
Inflammatory cytokine rate %
IFN-γ
IL-17
FoxP3
Sham
CLP+WT
CLP+CD4-STING-/-
Spleen
Inflammatory cytokine rate %
IFN-γ
IL-17
FoxP3
C
Sham
CLP+WT
CLP+CD4-STING-/-
14.8
27.4
15.1
15.4
30.7
14.8
22.4
10.5
20.3
CD4
IFN-γ
IL-17
FoxP3
D
naïve CD4 T+CD3/28 beads
CLP+WT
CLP+CD4-STING-/-
32.5
38.3
15.0
15.2
18.5
27.2
CD4
IFN-γ
IL-17
FoxP3
CLP+WT
CLP+CD4-STING-/-
Inflammatory cytokine rate %
IFN-γ
IL-17
FoxP3

◂**Fig. 4** STING promoted T cells differentiating into Th1/17. $CD4^+$ T cells-specific STING conditional knockout (CD4-$STING^{-/-}$) mice were subjected to CLP surgery, and WT mice as control. Post surgery 24 h, the spleen tissues and coronary blood samples were obtained for next analysis. **A**. Western blot and RT-qPCR assays were conducted to evaluated the expression of STING in $CD4^+$ T cells and $CD8^+$ T cells. **B**. The differentiation rate of $CD4^+$ T cells toward to Th1, Th17 and Treg cells in coronary blood samples were analyzed by flow cytometry. **C**. The differentiation rate of $CD4^+$ T cells toward to Th1, Th17 and Treg cells in spleen tissues were analyzed by flow cytometry. **D**. CD4 + T from WT or CD4-$STING^{-/-}$ mice were isolated for T cells differentiation test under indicating cytokine panel. **E**. ELISA was employed to detect the levels of inflammatory factors including IL-6, IL-1β, IL-12, TNF-α and IL- 10. **F**. Cardiac function parameters (LVEF, LVFS, LVESD) were evaluated by echocardiography. **G**. Representative images stained by HE for assessing the pathologic changes. Data was shown as mean ±SD. N = 5. *p < 0.05, **p < 0.01, ***p < 0.001

contributed to the pathogenesis of SCM by modulating $CD4^+$ T cells differentiation, indicating that inhibition of STING might be a promising potential strategy for SCM immunotherapy. Interestingly, some studies have found that LPS-induced myocardial injury can be related to the activation of STING pathway (Wang et al. 2021). The expression of STING in cardiomyocytes of specific knockout mice can improve the survival rate and cardiac function of myocardial mice induced by sepsis (Li et al. 2019). And inhibition of cGAS-STING-TBK1 signaling pathway can inhibit myocardial apoptosis and inflammatory reaction caused by bloody cardiac arrest (Zhou et al. 2025). These studies suggest that STING signaling pathway may also play a regulatory role in myocardial cells. Our study also proved the effect of STING signaling pathway on the differentiation of $CD4^+$ T cells related to myocardial injury. Therefore, we speculate that the direct effect of STING signaling pathway on myocardial cell injury and the effect of $CD4^+$ T cells differentiation have synergistic or superimposed effects. This will also be the focus of our follow-up research.

ELF4 was highly expressed in various hematopoietic cells, including natural killer (NK) cells, myeloid cells, T cells, and monocytes (Suico et al. 2017). As an innate immune molecule, ELF4 enhanced host resistance to malaria by activating transcription of two C-X-C chemokines (PPBP and PF4) (Wang et al. 2019), and promoted clearance of Staphylococcus aureus by macrophages via the lysosomal biogenesis pathway (Kang et al. 2021). Following viral infection, ELF4 was recruited by STING and interacted with the MAVS-TBK1 complex, translocating into the nucleus to induce innate immune signaling and antiviral defenses (Yamada et al. 2009). Despite these findings, there was few studies reporting the potential involvement of ELF4 in sepsis triggered by bacterial or viral infections. Here, we focused on the role of ELF4 in SCM. Encouragingly, we validated the interaction between ELF4 and STING in $CD4^+$ T cells. Lee et al. demonstrated that ELF4 knockdown promoted Th17 differentiation of $CD4^+$ T cells, exacerbating autoimmune encephalomyelitis severity (Lee et al. 2014). Concurrently, ELF4 had been shown to ameliorate inflammatory bowel disease by suppressing Th17 cells activity (Cao et al. 2023). ELF4 had also been implicated in promoting the development and function of memory $CD8^+$ T cells following Listeria monocytogenes infection (Mamonkin et al. 2014). Moreover, in tumors, ELF4 regulated $CD8^+$ T cells proliferation and homing by activating KLF4 and KLF2 (Yamada et al. 2009). These findings established that ELF4 was a crucial regulator of T cells immunity. In this study, we investigated the potential role of ELF4 in SCM through its modulation of T cells differentiation via the STING pathway. Our results showed that ELF4 directly interacted with STING and inhibited STING activation. And overexpression of ELF4 inhibited the differentiation of mouse $CD4^+$ T cells into Th1 and Th17 subsets, and increased their differentiation into Treg. T cells overexpressing ELF4 were adoptively transferred to CLP mice, which improved the myocardial injury of CLP mice. These findings suggested that ELF4 mediated immune imbalance through regulating STING signaling cascade in SCM progression. It was worth noting that ELF4 was reported to regulated inflammatory response caused by Staphylococcus aureus through inactivating mTOR signaling (Kang et al. 2021). Thus, we speculated that ELF4 may be involved in immune regulation and SCM progression by influencing other signaling pathways, which will require more studies to explore the molecular regulatory mechanisms involved in ELF4 in the future.

However, our study still has some limitations. Firstly, patient samples were missing from our study design. Besides, our detected sample was coronary

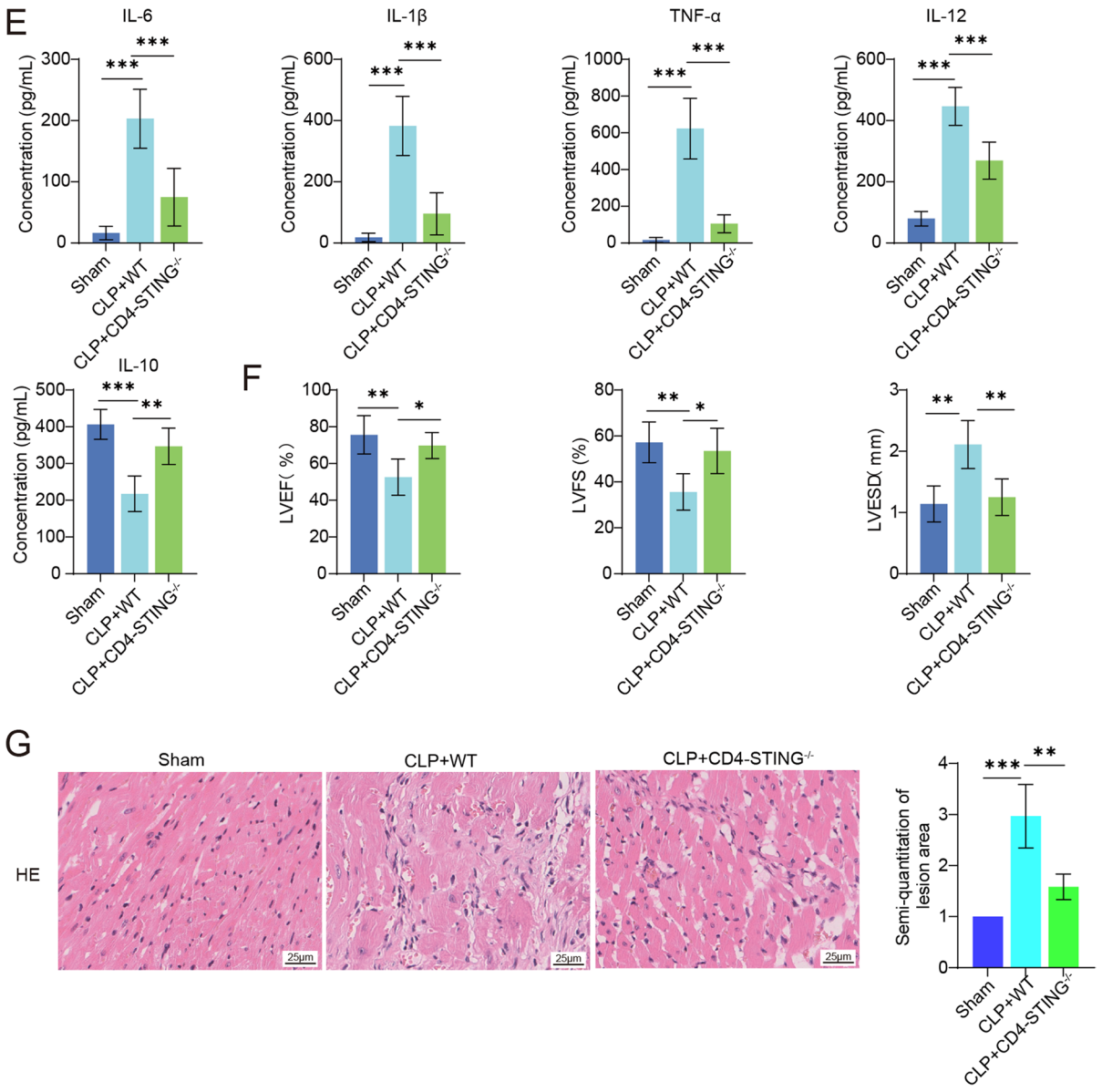

Fig. 4 (continued)

blood and heart tissue, however, T cells in peripheral blood were not detected. At present, most of the research mainly focuses on the direct injury of myocardial cells, including the increase of apoptosis caused by inflammatory reaction of myocardial cells directly caused by sepsis (Busch et al. 2021). The myocardial injury caused by immune cells in sepsis mainly includes increased neutrophil infiltration (Yang et al. 2021), natural killer T cells differentiation (Chen et al. 2023) and increased secretion of inflammatory factors caused by macrophage polarization (Chen et al. 2022c), which further stimulates myocardial cell injury. However, whether inflammatory factors secreted by myocardial cells due to inflammatory reaction can negatively regulate the differentiation of T cells and further aggravate sepsis and lead to myocardial injury also needs our in-depth study in the future.

Table 3 Echocardiographic properties feature of Fig. 4 experimental mice

	Sham (WT)	CLP + WT	CLP + CD4-STING-/-	CD4-STING-/-
Heart rate (bpm)	466.8 ± 8.96	474.2 ± 5.63	471.8 ± 6.22	466.4 ± 5.98
LV EF (%)	75.63 ± 10.40	52.61 ± 9.87	69.78 ± 7.11	72.60 ± 5.03
LV FS (%)	57.22 ± 8.88	35.61 ± 7.93	53.53 ± 9.87	54.80 ± 4.49
LV ESD (mm)	1.14 ± 0.29	2.11 ± 0.39	1.25 ± 0.30	1.06 ± 0.27
Calculated LV mass (mg)	92.06 ± 3.12	88.9 ± 2.07	90.56 ± 3.20	91.94 ± 1.92

Conclusion

In conclusion, these findings provide the first evidence that ELF4 promoted $CD4^+$ T cells differentiation into Treg cells while suppressing Th1 and Th17 differentiation by inactivation of the STING signaling, ultimately improving myocardial damage in SCM. Thus, selective modulation of the ELF4-STING signaling

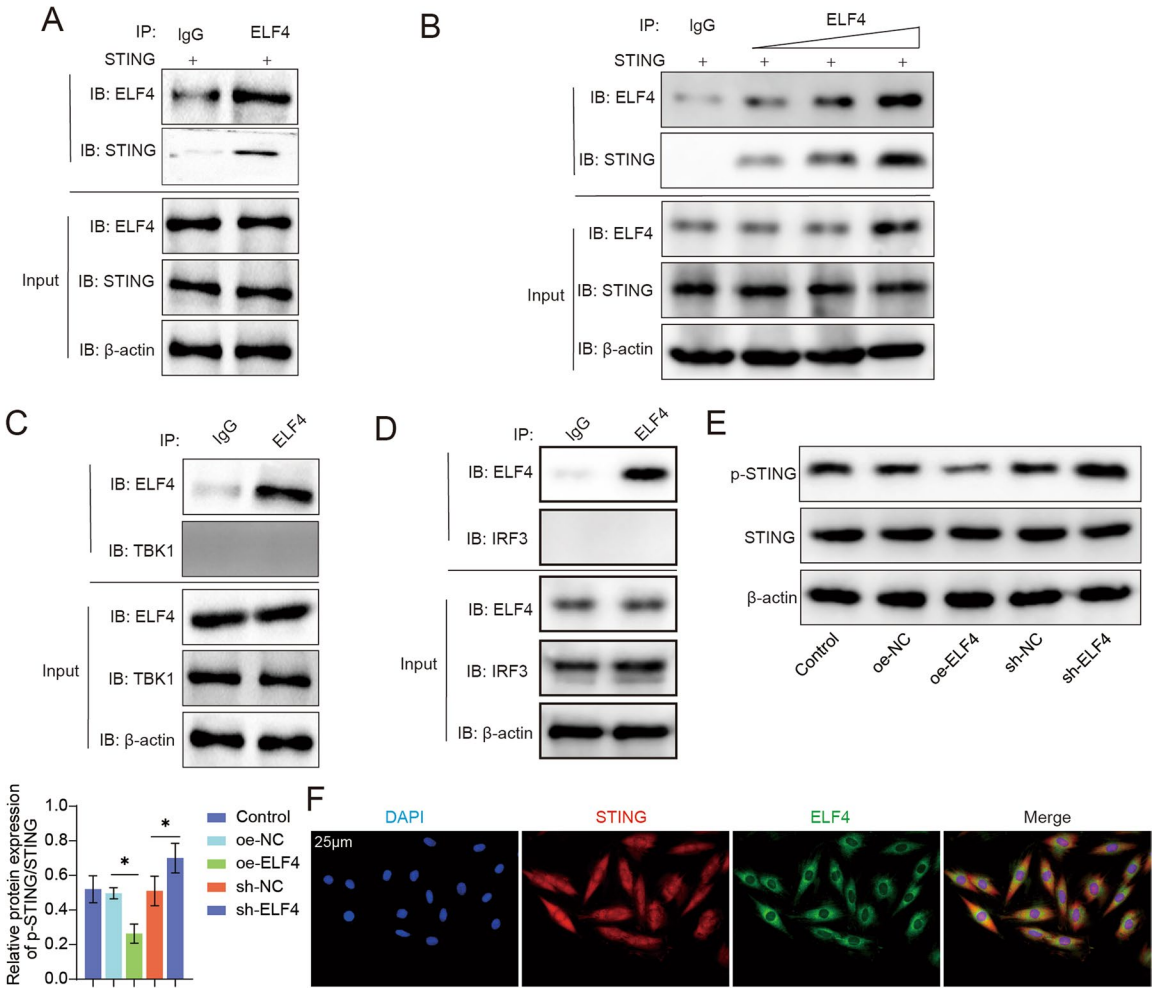

Fig. 5 ELK4 interacted with STING to inhibit the activation of STING in $CD4^+$ T cells. **A-E**. 293T was transfected by STING plasmid. **A-D.** Co-IP experiment verified the direct interaction between ELF4 and STING in 293T. The interaction between ELF4 and TBK1 or IRF3 was also evaluated by Co-IP experiment. **E**. 293T were transfected with oe-ELF4, sh-ELF4 or corresponding NCs. The protein levels of STING and p-STING were detected by western blot assay. **F**. The confocal co-localization images of STING and ELF4 in 293T. Data was shown as mean ± SD. N = 3. *p < 0.05

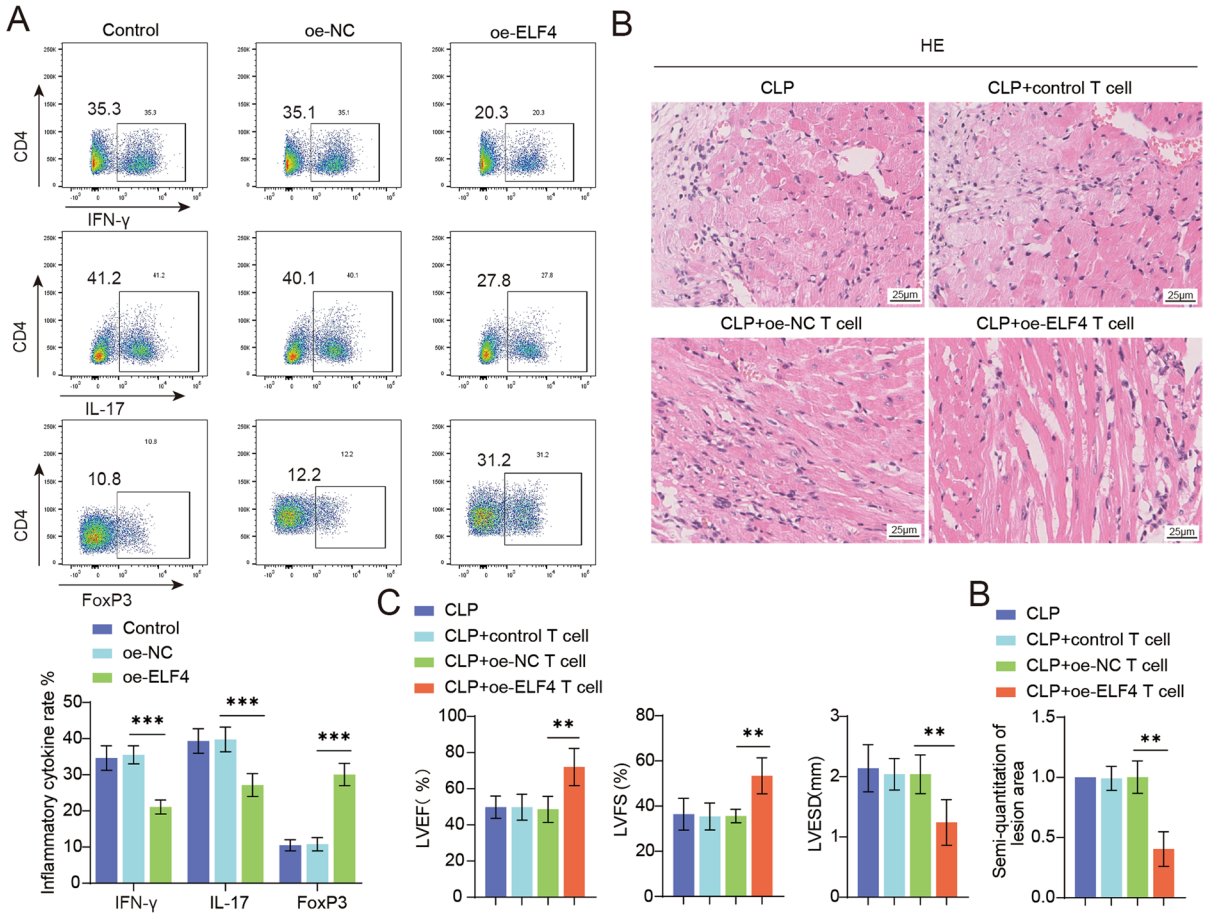

Fig. 6 ELF4 overexpression alleviated cardiomyocyte injury by suppressing STING signaling-mediated Th1/17 differentiation**. A.** Mouse primary $CD4^+$ T cells were isolated and transfected with overexpressing ELF4 plasmids for differentiation test ex vivo. The proportion of Th1, Th17 and Treg were detected by flow cytometry. **B**. Undifferentiated control T cells, OE-NC T cells, and OE-ELF4 T cells were adoptively transferred into WT mice, followed by CLP surgery. Representative images stained by HE for assessing the pathologic changes. **C**. Echocardiography was used to evaluate cardiac function parameters (LVEF, LVFS, LVESD). Data was shown as mean ± SD. N = 5. **p < 0.01, ***p < 0.001

Table 4 Echocardiographic properties feature of Fig. 6 experimental mice

	CLP	CLP + control T cell	CLP + oe-NC T cell	CLP + oe-ELF4 T cell
Heart rate (bpm)	473.2 ± 7.22	471.8 ± 9.23	475 ± 6.20	471 ± 2.92
LV EF (%)	49.80 ± 6.14	49.80 ± 7.16	48.60 ± 7.20	72 ± 10.30
LV FS (%)	36.40 ± 7.02	35.40 ± 5.94	35.60 ± 2.97	53.40 ± 7.99
LV ESD (mm)	2.14 ± 0.39	2.04 ± 0.26	2.04 ± 0.32	1.24 ± 0.38
Calculated LV mass (mg)	87.6 ± 4.10	86.78 ± 5.02	86.34 ± 3.50	90.78 ± 3.33

axis might be a viable therapeutic strategy for SCM treatment.

Acknowledgements Not applicable.

Authors'contributions Yawen Zheng: Conceptualization, Investigation, Methodology, Validation, Data Curation, Formal analysis, Writing—Original Draft and Writing—Review & Editing. Xiongjun Peng: Resources, Validation, Data Curation, Formal analysis and Writing—Original Draft. Yusha Zhang: Resources, Validation, Data Curation, Formal analysis and Software. Ruilin Liu: Resources, Validation, Data Curation, Formal analysis and Visualization. Junke Long: Conceptualization, Investigation, Methodology, Formal analysis, Project administration, Supervision, Writing—Original Draft and Writing—Review & Editing. All authors read and approved the final manuscript.

Funding This study is supported by the National Natural Science Foundation of China (No. 82100314).

Data availability All data generated or analysed during this study are included in this article. The datasets used and/or analysed during the current study are available from the corresponding author on reasonable request.

Declarations

Ethical approval The animal use protocol listed has been reviewed and approved by the Institutional Animal Care and Use Committee (IACUC) of The Second Xiangya Hospital, Central South University (No. 2021229).

Conflict of interest The authors declare no competing interests.

References

Anyalebechi JC, et al. CD8(+) T cells are necessary for improved sepsis survival induced by CD28 agonism in immunologically experienced mice. Front Immunol. 2024;15:1346097.

Benoit-Lizon I, et al. CD4 T cell-intrinsic STING signaling controls the differentiation and effector functions of T(H)1 and T(H)9 cells. J Immunother Cancer. 2022;10(1):e003459.

Berger G, et al. STING activation promotes robust immune response and NK cell-mediated tumor regression in glioblastoma models. Proc Natl Acad Sci U S A. 2022;119(28):e2111003119.

Busch K, et al. Inhibition of the NLRP3/IL-1beta axis protects against sepsis-induced cardiomyopathy. J Cachexia Sarcopenia Muscle. 2021;12(6):1653–68.

Cao M, et al. The transcription factor ELF4 alleviates inflammatory bowel disease by activating IL1RN transcription, suppressing inflammatory TH17 cell activity, and inducing macrophage M2 polarization. Front Immunol. 2023;14:1270411.

Chaturvedi V, et al. T-cell activation profiles distinguish hemophagocytic lymphohistiocytosis and early sepsis. Blood. 2021;137(17):2337–46.

Chen F, et al. The STING1-MYD88 complex drives ACOD1/IRG1 expression and function in lethal innate immunity. iScience. 2022a;25(7):104561.

Chen J, et al. Early Expression of Functional Markers on CD4(+) T Cells Predicts Outcomes in ICU Patients With Sepsis. Front Immunol. 2022b;13:938538.

Chen XS, et al. Losartan attenuates sepsis-induced cardiomyopathy by regulating macrophage polarization via TLR4-mediated NF-kappaB and MAPK signaling. Pharmacol Res. 2022c;185:106473.

Chen LR, et al. CD1d-dependent natural killer T-cells inactivation aggravates sepsis-induced myocardial injury via T lymphocytes infiltration and IL-6 production in mice. Int Immunopharmacol. 2023;120:110256.

Danahy DB, et al. Clinical and Experimental Sepsis Impairs CD8 T-Cell-Mediated Immunity. Crit Rev Immunol. 2016;36(1):57–74.

Gu X, et al. Respiratory viral sepsis: epidemiology, pathophysiology, diagnosis and treatment. Eur Respir Rev. 2020;29(157):200038.

Heidarian M, Griffith TS, Badovinac VP. Sepsis-induced changes in differentiation, maintenance, and function of memory CD8 T cell subsets. Front Immunol. 2023;14:1130009.

Huang S, et al. Tim-3 regulates sepsis-induced immunosuppression by inhibiting the NF-κB signaling pathway in CD4 T cells. Mol Ther. 2022;30(3):1227–38.

Imanishi T, et al. Nucleic acid sensing by T cells initiates Th2 cell differentiation. Nat Commun. 2014;5:3566.

Imbaby S, Hattori Y. Stattic ameliorates the cecal ligation and puncture-induced cardiac injury in septic mice via IL-6-gp130-STAT3 signaling pathway. Life Sci. 2023;330:122008.

Jensen IJ, et al. Sepsis-induced T cell immunoparalysis: the ins and outs of impaired T cell immunity. J Immunol. 2018;200(5):1543–53.

Jneid B, et al. Selective STING stimulation in dendritic cells primes antitumor T cell responses. Sci Immunol. 2023;8(79):eabn6612.

Kang Y, et al. Elf4 regulates lysosomal biogenesis and the mTOR pathway to promote clearance of Staphylococcus aureus in macrophages. FEBS Lett. 2021;595(7):881–91.

Kuroshima T, Kawaguchi S, Okada M. Current perspectives of mitochondria in sepsis-induced cardiomyopathy. Int J Mol Sci. 2024;25(9):4710.

Lee PH, et al. The transcription factor E74-like factor 4 suppresses differentiation of proliferating CD4+ T cells to the Th17 lineage. J Immunol. 2014;192(1):178–88.

Lee GW, et al. Supraphysiological Levels of IL-2 in Jak3-Deficient Mice Promote Strong Proliferative Responses of Adoptively Transferred Naive CD8(+) T Cells. Front Immunol. 2020;11:616898.

Li N, et al. STING-IRF3 contributes to lipopolysaccharide-induced cardiac dysfunction, inflammation, apoptosis and pyroptosis by activating NLRP3. Redox Biol. 2019;24:101215.

Liu P, et al. Baicalin suppresses Th1 and Th17 responses and promotes Treg response to ameliorate sepsis-associated pancreatic injury via the RhoA-ROCK pathway. Int Immunopharmacol. 2020;86:106685.

Liu S, et al. Tim-3 Blockade Decreases the Apoptosis of CD8(+) T Cells and Reduces the Severity of Sepsis in Mice. J Surg Res. 2022;279:8–16.

Liu H, et al. ALDH2 mitigates LPS-induced cardiac dysfunction, inflammation, and apoptosis through the cGAS/STING pathway. Mol Med. 2023;29(1):171.

Long J, et al. Notch signaling protects CD4 T cells from STING-mediated apoptosis during acute systemic inflammation. Sci Adv. 2020;6(39):eabc5447.

Luan YY, et al. STING modulates necrotic cell death in CD4 T cells via activation of PARP-1/PAR following acute systemic inflammation. Int Immunopharmacol. 2022;109:108809.

Mamonkin M, Puppi M, Lacorazza HD. Transcription factor ELF4 promotes development and function of memory CD8(+) T cells in Listeria monocytogenes infection. Eur J Immunol. 2014;44(3):715–27.

Niu R, et al. Ouabain attenuates sepsis-induced immunosuppression in mice by activation and anti-apoptosis of T cells. Med Sci Monit. 2018;24:2720–7.

Oser MG, et al. The KDM5A/RBP2 histone demethylase represses NOTCH signaling to sustain neuroendocrine differentiation and promote small cell lung cancer tumorigenesis. Genes Dev. 2019;33(23–24):1718–38.

Ratiu JJ, et al. Loss of Zfp335 triggers cGAS/STING-dependent apoptosis of post-β selection thymocytes. Nat Commun. 2022;13(1):5901.

Rudd KE, et al. Global, regional, and national sepsis incidence and mortality, 1990–2017: analysis for the Global Burden of Disease Study. Lancet. 2020;395(10219):200–11.

Suico MA, Shuto T, Kai H. Roles and regulations of the ETS transcription factor ELF4/MEF. J Mol Cell Biol. 2017;9(3):168–77.

Tyler PM, et al. Human autoinflammatory disease reveals ELF4 as a transcriptional regulator of inflammation. Nat Immunol. 2021;22(9):1118–26.

van der Poll T, Shankar-Hari M, Wiersinga WJ. The immunology of sepsis. Immunity. 2021;54(11):2450–64.

Wang D, et al. ELF4 facilitates innate host defenses against plasmodium by activating transcription of Pf4 and Ppbp. J Biol Chem. 2019;294(19):7787–96.

Wang X, et al. Selenium supplementation protects against lipopolysaccharide-induced heart injury via sting pathway in mice. Biol Trace Elem Res. 2021;199(5):1885–92.

Wu J, et al. STING-mediated disruption of calcium homeostasis chronically activates ER stress and primes T cell death. J Exp Med. 2019;216(4):867–83.

Wu B, et al. STING inhibitor ameliorates LPS-induced ALI by preventing vascular endothelial cells-mediated immune cells chemotaxis and adhesion. Acta Pharmacol Sin. 2022;43(8):2055–66.

Xia XJ, et al. Preoperative CD4 count or CD4/CD8 ratio as a useful indicator for postoperative sepsis in HIV-infected patients undergoing abdominal operations. J Surg Res. 2012;174(1):e25-30.

Xia H, et al. Maresin1 ameliorates acute lung injury induced by sepsis through regulating Th17/Treg balance. Life Sci. 2020;254:117773.

Yamada T, et al. Transcription factor ELF4 controls the proliferation and homing of CD8+ T cells via the Krüppel-like factors KLF4 and KLF2. Nat Immunol. 2009;10(6):618–26.

Yang Y, et al. gammadelta T/Interleukin-17A contributes to the effect of maresin conjugates in tissue regeneration 1 on lipopolysaccharide-induced cardiac injury. Front Immunol. 2021;12:674542.

You F, et al. ELF4 is critical for induction of type I interferon and the host antiviral response. Nat Immunol. 2013;14(12):1237–46.

Zhang X, Bai XC, Chen ZJ. Structures and mechanisms in the cGAS-STING innate immunity pathway. Immunity. 2020;53(1):43–53.

Zhao GJ, et al. Supplementation with nicotinamide riboside attenuates t cell exhaustion and improves survival in sepsis. Shock. 2023;60(2):238–47.

Zhou T, et al. Dl-3-N-Butylphthalide alleviates cardiac dysfunction and injury possibly by inhibiting cell pyroptosis and inflammation via the Cgas-Sting-Tbk1 pathway in a porcine model of hemorrhage-induced cardiac arrest. Shock. 2025;63(4):614–21.